Journal of Physics: Conference Series **665** (2016) 012035 doi:10.1088/1742-6596/665/1/012035

High precision elastic α scattering on the even-odd ^{115}In nucleus at low energies

G G Kiss[1], T Szücs[1], P Mohr[1,2], Zs Fülöp[1], Gy Gyürky[1], Z Halász,[1,3], R F Soha[4], E Somorjai[1], A Ornelas[5], D. Galaviz[5], C Yalçın[1,6], R T Güray[6], N Özkan[6]

[1] Institute for Nuclear Research (ATOMKI), H-4001 Debrecen, POB.51., Hungary
[2] Diakonie-Klinikum, D-74523 Schwäbisch Hall, Germany
[3] University of Debrecen, Department of Theoretical Physics, H-4001 Debrecen, Hungary
[4] University of Debrecen, Department of Solid State Physics, H-4010 Debrecen, Hungary
[5] Centro de Física Nuclear da Universidade de Lisboa, 1649-003, Lisbon, Portugal
[6] Kocaeli University, Department of Physics, TR-41380 Umuttepe, Kocaeli, Turkey

E-mail: ggkiss@atomki.mta.hu

Abstract. Elastic alpha scattering cross sections on the even-odd ^{115}In nucleus have been measured at energies $E_{lab.}$ = 16.15 MeV and 19.50 MeV. The high precision experimental data are used to derive the parameters of a local α nucleus optical potential.

1. Introduction

Studies in the fields of nuclear structure, nuclear reaction theory, and nuclear astrophysics require the knowledge of α+nucleus optical model potentials (OMP). For example, the OMP plays a role in the determination of the α-decay half-lives of superheavy nuclei [1, 2], and in the unification of the bound and scattering α-particle states [3]. Furthermore, in several astrophysical applications – such as modeling the nucleosynthesis in explosive scenarios like the γ process – the reaction rates are taken from the Hauser-Feshbach (H-F) statistical model [4] using global OMPs [5, 6].

The optical potential combines a Coulomb term with the complex form of the nuclear potential, which consists of a real and an imaginary part. Usually, the parameters of the OMP are derived from the analysis of the angular distributions of elastically scattered α-particles (and are adjusted to experimental α-induced cross sections if they are known).

The variation of the potential parameters of the real part as a function of mass and energy is smooth and relatively well understood [7]. On the contrary, the imaginary part of the optical potential is strongly energy-dependent, especially at energies around the Coulomb barrier. In astrophysical applications the parameters of the OMP have to be known at energies well below the Coulomb barrier. However, at such energies the α+nucleus elastic scattering cross section is non-diffractive and dominated by the Rutherford component. Therefore, the elastic α scattering experiments have to be carried out at slightly higher energies with high precision. From the analysis of the measured angular distributions the parameters of the potential can be derived and have to be extrapolated down to the astrophysically relevant energy region where the relevant α-particle induced-reactions are taking place.


Content from this work may be used under the terms of the Creative Commons Attribution 3.0 licence. Any further distribution of this work must maintain attribution to the author(s) and the title of the work, journal citation and DOI.
Published under licence by IOP Publishing Ltd

Several α elastic scattering experiments on the target nuclei ^{89}Y, ^{92}Mo, ^{106,110,116}Cd, ^{112,124}Sn, and ^{144}Sm have been performed at ATOMKI in recent years [8-13]. A summary of these works is given in [14, 15]. Previously either semi-magic or even-even target nuclei were investigated. In all of these cases complete angular distributions have been measured at energies close to the Coulomb barrier. The chosen energies were low enough to be close to the region of astrophysical interest and high enough that the scattering cross section differs sufficiently from the Rutherford cross section. This work presents the elastic scattering experiment performed on the ^{115}In non-magic, even-odd nucleus to study further the behavior of the optical potentials at low energies.

2. Experimental technique

The experiment was carried out at the cyclotron laboratory of ATOMKI, Debrecen. A similar experimental setup was used in previous experiments (see e.g. [11]). The following paragraphs provide only a short description of the experimental setup.

The targets for the alpha scattering experiment were made by vacuum evaporation of natural high chemical purity (99.99%) In onto 40 μg/cm^2 thick C foils. During the evaporation, the C backings were fixed in a holder placed 10 cm above the Ta evaporation boat. The target thickness was determined by α energy loss measurment and was found to be $\approx$ 95 μg/cm^2. The energy of the alpha beam provided by the cyclotron accelerator of ATOMKI was E_{lab} = 16.15 and 19.50 MeV (corresponding to $E_{c.m.}$ = 15.59 and 18.83 MeV, after taking into account the energy loss in the target, which is about 15 keV), with a beam current of 150 pnA. The beam enters the scattering chamber through a complex collimator system, necessary to have a point-like beamspot ($\leq$ 4mm^2) at well-defined beam energy (energy spread $\leq$ 100 keV) which is needed for the precise determination of the scattering angle and for fixing the energy dependence of the imaginary potential.

There are two independently rotatable turntables, each of them are holding two (used to scan the forward angular region) or five (used to measure the yield of the scattered alpha particles above $\geq 100^\circ$) Ion Implanted Silicon Detectors. The thickness of the detectors is 500 μm, and their solid angles vary within $\Delta\Omega$ = 1.0 x 10^{-4} and 1.6 x 10^{-4}. To reach stable operation with higher angular precision and repeatability the mechanical transmission of the scattering chamber was redesigned. The formerly used motors were replaced by 3-phase hybrid stepper motors [17] and closed-loop drives [18] to allow 0.006° stepsize precision and avoid step loss. The system was remote controlled via Labview development environment [19] and all the operations were documented for later analysis.

In addition, two detectors were mounted at a larger distance on the wall of the scattering chamber at fixed angles of 15° left and right to the beam axis. These detectors were used as monitor detectors during the experiment to normalize the measured angular distributions, to determine precisely the beam position on the target and to monitor the target thickness. The solid angle of these detectors are $\Delta\Omega$ = 8.2 x 10^{-6}.

Knowledge on the exact angular position of the detectors is of crucial importance for the precision of a scattering experiment because the Rutherford cross section depends sensitively on the angle. The uncertainty in the angular distribution is dominated by the error of the scattering angles in the forward region. A tiny uncertainty of $\Delta\vartheta = 0.3^\circ$ results in a significant error of approximately 5% in the Rutherford normalized cross sections at very forward angles.

To determine the scattering angle precisely, — similarly to [11] — we measured kinematic coincidences between elastically scattered α particles and the corresponding ^{12}C recoil nuclei using a pure carbon foil target. As the result of this procedure the final angular uncertainty was found to be $\leq 0.13^\circ$ for each detector.

Typical spectra are shown in Fig. 1. The relevant peaks from elastic ^{115}In - α scattering are well separated from elastic and inelastic peaks of target contaminations, and — as expected — peaks from inelastic α scattering on ^{115}In are not visible. The energy of the first excited state

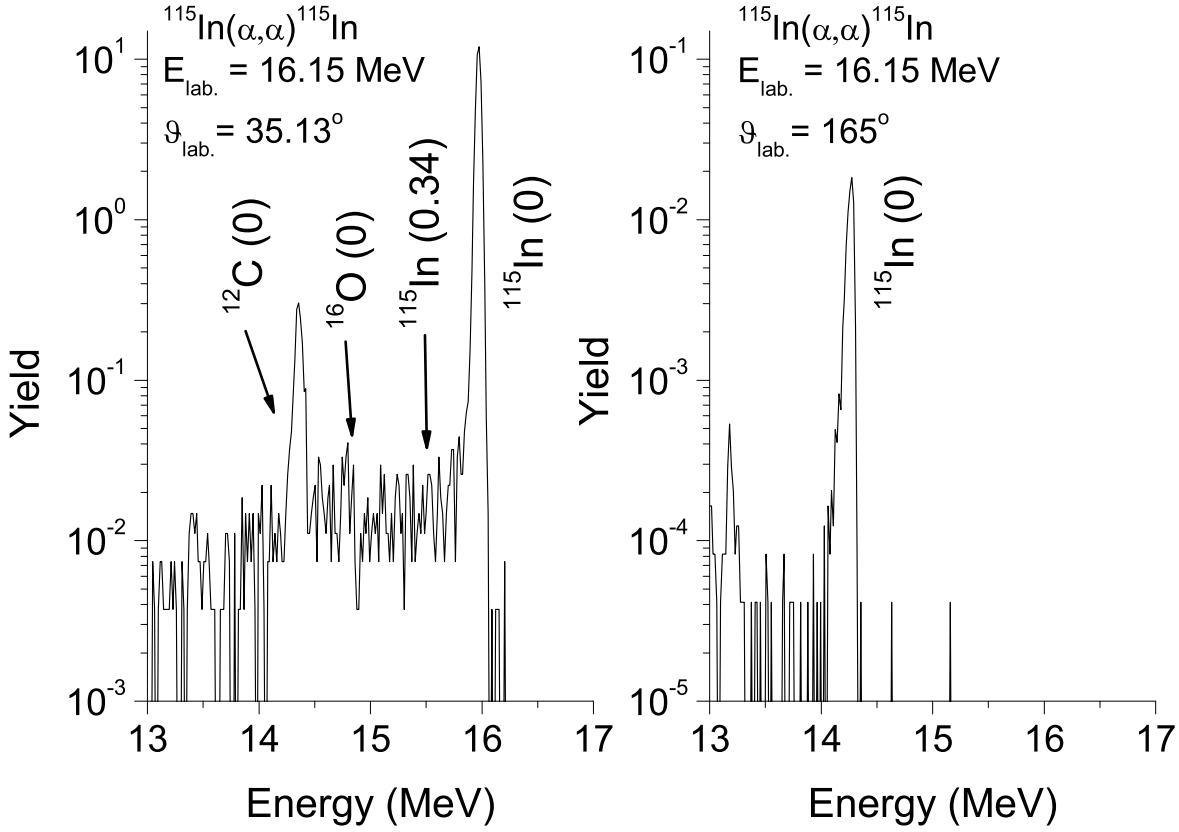


Figure 1. Typical spectra taken at E_{lab} = 16.15 MeV at ϑ = 35.13° and 165.05°. The peak from elastic ^{115}In-α scattering is well resolved from both the ^{12}C-α and ^{16}O-α elastic scattering.

of the ^{115}In nucleus is 336.24 keV. There is a large difference between the spin of the ground and the first excited states ($9/2^+$ and $1/2^-$ respectively) [16], therefore the expected inelastic scattering cross section is very low at the measured energies. This fact explains why events corresponding to inelastic α scattering on ^{115}In are missing from the spectra.

3. Experimental results and the optical potential study

Complete angular distributions between 20° and 175° were measured at energies of E_α = 16.15 and 19.5 MeV in 1° ($20° \leq \vartheta \leq 100°$), and 2.5° ($100° \leq \vartheta \leq 175°$) steps. The count rates $N(\vartheta)$ have been normalized to the yield of the monitor detectors $N_{Mon}(\vartheta=15°)$

$$\left(\frac{d\sigma}{d\Omega}\right)(\vartheta) = \left(\frac{d\sigma}{d\Omega}\right)_{Mon} \frac{N(\vartheta)}{N_{Mon}} \frac{\Delta\Omega_{Mon}}{\Delta\Omega}, \quad (1)$$

with $\Delta\Omega$ being the solid angles of the detectors. The cross section at the position of the monitor detectors is taken as pure Rutherford. The relative measurement eliminates the typical uncertainties of absolute measurements, coming mainly from changes in target and from the beam current integration.

The measured Rutherford-normalized angular distributions are shown in Fig.2. The experimental absolute cross sections cover five orders of magnitude between the highest (forward angles at E_α=16.15 MeV) and the lowest cross sections (backward angle at E_α=19.5 MeV)

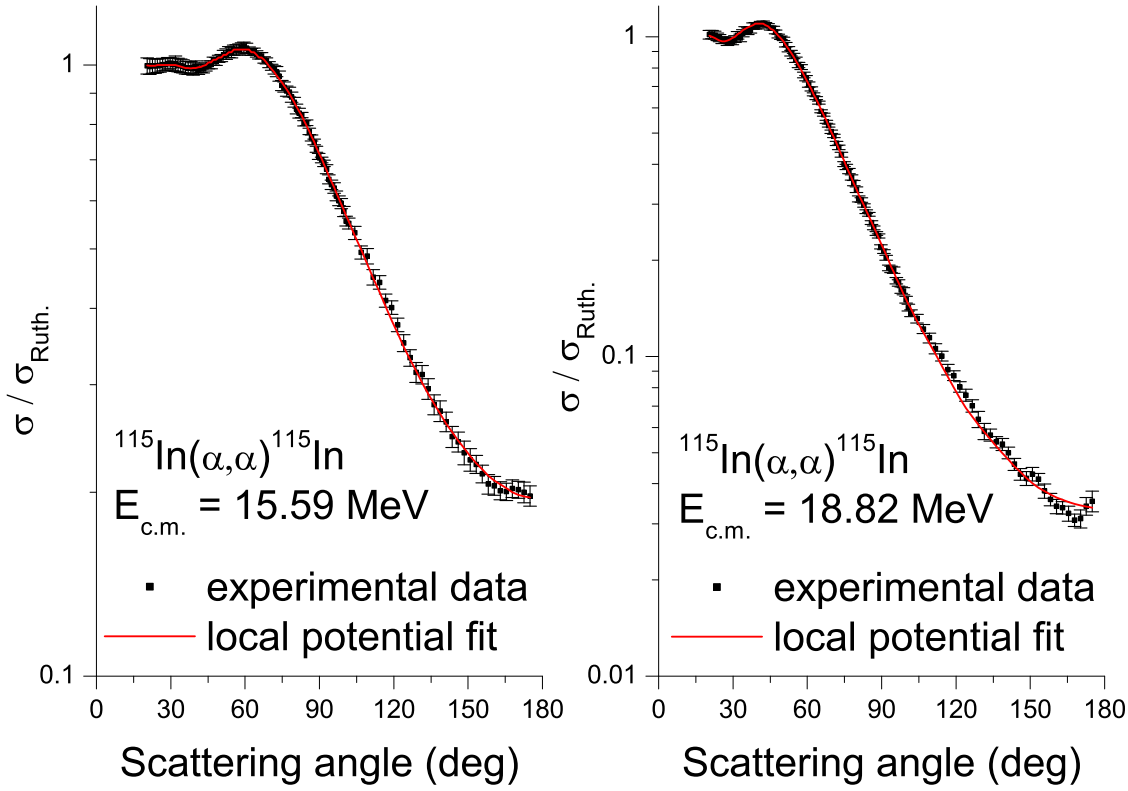


Figure 2. Rutherford normalized elastic scattering cross sections of ^{115}In$(\alpha,\alpha)^{115}$In reaction at $E_{c.m.}$ = 15.59 and 18.83 MeV versus the angle in center-of-mass frame. The lines correspond to the predictions using the local optical potential parameter set derived in the present work (and listed in Tab.2). Note the different scale of the two figures.

with almost the same accuracy (4-5% total uncertainty). This error is mainly caused by the uncertainty of the determination of the scattering angle in the forward region and by the statistical uncertainty in the backward region. The lines correspond to the result of optical model calculations using the local α-nucleus potential, its parameters are listed in Table 2.

The real part $V(r)$ of the nuclear potential is determined by a double-folding procedure using the densities of the α projectile and ^{115}In target (derived from electron scattering [20]) with an effective nucleon-nucleon interaction of the widely used DDM3Y type [21, 22] (for details of the folding procedure see also [23, 14]). The bare folding potential $V_F(r)$ is modified by a strength parameter λ and a width parameter w

$$V(r) = \lambda\, V_F(r/w) \quad . \tag{2}$$

The strength parameter λ and the width parameter w are adjusted to the experimental ^{115}In$(\alpha,\alpha)^{115}$In elastic scattering angular distributions. The width parameter w should remain close to unity and the strength parameter λ is typically around $1.1 - 1.4$ [7].

The Coulomb potential $V_C(r)$ is taken as usual from a homogeneously charged sphere, with the radius parameter R_C taken from the root-mean-square (rms) radius of the bare folding potential (with $w = 1$).

Table 1. Parameters of the local optical potential derived in the present work.

$E_{c.m.}$ MeV	λ	w	J_R MeV fm^3	r_R fm	W_s MeV	R_s fm	a_s fm	J_I MeV fm^3	r_I fm	χ^2_{red}
15.59	1.3001	0.99781	342.20	5.314	143.77	1.4658	0.3996	80.56	7.310	0.268
18.82	1.4120	0.99193	365.14	5.283	162.59	1.4175	0.4526	96.89	7.133	0.926

The imaginary potential $W(r)$ is parameterized by Woods-Saxon potentials of volume and surface type:

$$W(r) = W_V f(x_V) + W_S \frac{df(x_S)}{dx_S} \quad . \tag{3}$$

The W_i are the depth parameters of the volume and surface imaginary potential, and the Woods-Saxon function $f(x_i)$ is given by

$$f(x_i) = \left[1 + \exp\left(x_i\right)\right]^{-1} \tag{4}$$

with $x_i = (r - R_i A_T^{1/3})/a_i$ and $i = V, S$ for the volume and surface part.

In general, at energies far above the Coulomb barrier the volume contribution is dominating whereas at lower energies the surface component becomes more important. The experimental energies of 15.59 MeV and 18.82 MeV are around the Coulomb barrier, therefore it is sufficient to neglect the volume contribution ($W_V = 0$) and to use a pure surface imaginary potential. The parameters of the local potential fits are listed in Table 1. The derived local alpha nucleus optical potential parameters were used to calculate the total reaction cross sections, σ_{reac} [15], which was found to be 350.5 ± 10.6 mb at $E_{c.m.}$=15.59 MeV and 777.0 ± 23.5 mb at $E_{c.m.}$=18.82 MeV, respectively.

4. Conclusions

Elastic ^{115}In(α,α)^{115}In scattering data have been measured at energies around the Coulomb barrier with high precision over the full angular range. A local optical potential has been derived from the new experimental data, and the new data will also be used to obtain an update of the global ATOMKI-V1 potential [14].

Acknowledgments

This work was supported by the EUROGENESIS research program, by the HUNGARIAN PORTUGUESE INTERGOVERNMENTAL S&T COOPERATION PROGRAMME NO. TÉT_10-1-2011-0458, by the European Research Council grant agreement no. 203175, by OTKA (NN83261, K101328, PD104664, K108459), by the Scientific and Technical Research Council of Turkey (TUBITAK, grant number: 109T585). G. G. Kiss acknowledges support from the János Bolyai Research Scholarship of the Hungarian Academy of Sciences. C. Yalçın acknowledges support through The Scientific and Technical Research Council of Turkey (TUBITAK) grant numbers: BIDEP-2219.

References

[1] V.Yu. Denisov, H. Ikezoe, 2005 *Phys. Rev.* C **72** 064613
[2] P. Mohr, 2006 *Phys. Rev.* C **73** 031301(R); 2006 *Phys. Rev.* C **74** 069902
[3] P.E. Hodgson 1990 *Contemp. Phys.* **31** 295
[4] W. Hauser and H. Feshbach, 1952 *Phys. Rev.* **87** 366
[5] T. Rauscher and F.-K. Thielemann 2000 *At. Data Nucl. Data Tables* **75** 1
[6] T. Rauscher and F.-K. Thielemann 2001 *At. Data Nucl. Data Tables* **79** 47
[7] U. Atzrott, P. Mohr, H. Abele, C. Hillenmayer, G. Staudt 1996 *Phys. Rev.* C **53** 1336

[8] G. G. Kiss, P. Mohr, Zs. Fülöp, D. Galaviz, Gy. Gyürky, Z. Elekes, E. Somorjai, A. Kretschmer, K. Sonnabend, A. Zilges and M. Avrigeanu 2009 *Phys. Rev. C* **80** 045807
[9] Zs. Fülöp, Gy. Gyürky, Z. Máté, E. Somorjai, L. Zolnai, D. Galaviz, M. Babilon, P. Mohr, A. Zilges, T. Rauscher, H. Oberhummer and G. Staudt 2001 *Phys. Rev.* C **64** 065805
[10] G. G. Kiss, Zs. Fülöp, Gy. Gyürky, Z. Máté, E. Somorjai, D. Galaviz, A. Kretschmer, K. Sonnabend and A. Zilges 2006 *Eur. Phys. J.* A **27** 197
[11] G. G. Kiss, P. Mohr, Zs. Fülöp, Gy. Gyürky, Z. Elekes, J. Farkas, E. Somorjai, C. Yalçın, D. Galaviz, R. T. Güray, N. Özkan and J. Görres 2011 *Phys. Rev.* C **83** 065807
[12] D. Galaviz, Zs. Fülöp, Gy. Gyürky, Z. Máté, P. Mohr, T. Rauscher, E. Somorjai and A. Zilges 2005 *Phys. Rev.* C **71** 065802
[13] P. Mohr, T. Rauscher, H. Oberhummer, Z. Máté, Zs. Fülöp, E. Somorjai, M. Jaeger and G. Staudt 1997 *Phys. Rev.* C **55** 1523
[14] P. Mohr, G. G. Kiss, Zs. Fülöp, D. Galaviz, Gy. Gyürky and E. Somorjai 2013 *At. Data Nucl. Data Tables* **99** 651
[15] P. Mohr, D. Galaviz, Zs. Fülöp, Gy. Gyürky, G. G. Kiss and E. Somorjai 2010 *Phys. Rev.* C **82** 047601
[16] J. Blanchot 2012 *Nuclear Data Sheets* **113** 2391
[17] 573S20-EC-100, Leadshine Technology Co., Ltd.
[18] HBS57 Stepper Motor Drive with Encoder Feedback, Leadshine Technology Co., Ltd.
[19] http://www.ni.com/labview/
[20] H. de Vries, C. W. de Jager and C. de Vries 1987 *At. Data and Nucl. Data Tables* **36** 495
[21] G. R. Satchler and W. G. Love 1979 *Phys. Rep.* **55** 183
[22] A. M. Kobos, B. A. Brown, R. Lindsay and G. R. Satchler 1984 *Nucl. Phys.* A **425** 205
[23] H. Abele and G. Staudt 1993 *Phys. Rev.* C **47** 742